doi: 10.56761/EFRE2024.N1-P-047301

Features of the structural-phase state and mechanical properties of titanium nickelide formed by electron beam wire-feed additive manufacturing using different strategies

A.A. Gusarenko, D.Y. Zhapova, K.V. Krukovskii, S.A. Martynov*

Institute of Strength Physics and Materials Science of SB RAS, Tomsk, Russia
aag@ispms.ru

Abstract. The study investigates the structural-phase state and mechanical properties of a TiNi-based alloy, printed by electron beam wire-feed additive manufacturing on a titanium substrate, using different printing strategies. It was shown that the printed samples have a heterogeneous coarse-grained microstructure. At room temperature, the printed samples, regardless of the printing strategy used, have the structure of the high-temperature B2 phase of TiNi and the secondary Ti_2Ni phase. It was established that printing samples using a strategy that involves contact with a larger area of the substrate leads to an increase in the diffusion of substrate atoms into the sample. In turn, this results in an increase in the volume fraction of the Ti_2Ni phase.
Keywords: electron beam wire-feed additive manufacturing, microstructure evolution, B2 phase state NiTi, microhardness.

1. Introduction

Alloys based on titanium nickelide (TiNi) have found wide application in medicine and engineering as materials exhibiting shape memory and superelastic effects [1, 2]. The interest in TiNi-based alloys is justified by the combination of their high physical-mechanical and unique functional properties (shape memory effect and superelasticity) [1, 3]. However, despite their versatility, TiNi-based alloys are difficult to process using traditional subtractive manufacturing methods due to high tool wear and labor-intensive machining stages of the workpieces. These difficulties are associated with the material's high specific heat capacity and its low thermal conductivity [4]. Therefore, the need for a practical method with lower production costs as well as high productivity has led to increased research interest in additive manufacturing as an effective method for producing custom products that have a close-to-design shape. The materials obtained in this way may potentially have variable compositions and properties.

Some of the popular TiNi AM methods are based on fusing alloyed or mixed powders with a laser beam, such as selective laser melting (SLM) and laser-based directed energy deposition (LB-DED). In particular, in [5, 6] it was shown that samples made from alloyed powder materials (particle size 25–75 μm) demonstrate up to 6–7% reversible deformation (with accumulation of plastic deformation ~ 1.5%) under compressive stresses of 1200 MPa. Additionally, study [7] demonstrated that by mixing Ti and Ni powders and using AM methods, bulk samples of the $Ti_{43}Ni_{57}$ (at. %) alloy can be obtained, which after high-temperature aging exhibit a sufficiently high value of superelasticity. However, as further experience with AM of powder materials has shown, such high values of inelastic properties can only be obtained from high-quality powders subject to strict storage and manufacturing conditions.

As a result, there has been an increased interest in electron beam wire-feed additive manufacturing (EBAM) [8, 9]. One of the features of the EBAM method is its use in a vacuum environment [8, 9, 10], which prevents contamination by oxygen, nitrogen, and carbon atoms. The disadvantages of the EBAM method include diffusion of substrate atoms (particularly Ti and Fe [11]) into the material of the formed samples. According to [12], in samples printed on a titanium substrate, there is a shift in composition towards equiatomic ratio and the precipitation of a secondary Ti_2Ni phase. However, annealing of printed samples at temperatures of 450–600 °C for 20 hours result in a more uniform distribution of Ti atoms throughout the sample and improves functional properties [12].

In this paper, we will study samples printed using EBAM method with subsequent cooling from 800 °C over two days. It is assumed that gradual cooling from high temperatures will create a more favorable structural-phase state for the functional properties of the printed samples. The aim of this work was to investigate the structural-phase state and mechanical properties of TiNi-based alloy printed by EBAM method on a titanium substrate using different printing strategies.

2. Materials and methods

The VT1-0 (Grade2) titanium plate with thickness of 5 mm was used as the substrate material. The $Ti_{49.3}Ni_{50.7}$ (at.%) alloy wire with a diameter of 1.2 mm was chosen as the raw material. The samples were printed on an EBAM machine using two strategies: thin-walled samples and bar-shaped samples. The thin-walled samples had dimensions of 25 mm in height, 30 mm in length, and 5 mm in width. The bar-shaped samples had dimensions of 15 mm in height, 30 mm in length, and 25 mm in width.

The investigations of the microstructure and phase state of the printed samples have been carried out using the equipment of Share Use Centre "Nanotech" of the ISPMS SB RAS (Tomsk, Russia). The structural-phase state of the samples was studied by X-ray diffraction analysis using a DRON-7 diffractometer at room temperature (CuKα radiation). The microstructure and phase composition of the printed samples were studied using a high-resolution field emission scanning electron microscope (HR FESEM) Apreo 2 S (Thermo Fisher Scientific, Waltham, Massachusetts, United States), equipped with Octane Elect Super energy-dispersive spectral analysis (EDS) detector (EDAX, Mahwah, New Jersey, United States) and Velocity Super (EDAX, Mahwah, New Jersey, United States) electron backscatter diffraction (EBSD) detector. The microhardness of the printed samples was studied using a universal hardness testing machine "Duramin-500" (Stuers A/S, Denmark) with an automatic Vickers and Rockwell force sensor.

3. Results and discussion

3.1. Microstructure

The samples obtained by the EBAM method have a heterogeneous grain structure, as shown in Fig. 1. Note that, regardless of the printing strategy, the studied samples have a qualitatively similar structure. As can be seen from the EBSD map, Fig. 1, equiaxed grains (from 1 to 60 μm in size) are formed at the boundary of the layers of the printed samples. Inside the layer, grains are formed that are elongated parallel to the printing direction (the printing direction from the substrate is shown in Fig. 1). This is due to the temperature gradient within the material layer. The size of the elongated grains is 50–150 μm in width and reaches 500–700 μm in length, Fig. 1.

X-ray diffraction analysis of the samples revealed that at room temperature, all printed samples, regardless of the printing strategy, are in the B2 phase state with a high proportion of the Ti_2Ni phase.

Fig. 2 shows fragment of the microstructure of thin-walled samples obtained by the secondary electron method. It can be seen that there are fragments of the secondary phase inside the grains. Studies by EBSD method have shown that thin-walled samples consist of a B2 phase of TiNi (highlighted in red) and the Ti_2Ni phase (highlighted in green), Fig. 3. The Ti_2Ni phase was formed due to the diffusion of Ti atoms from the substrate. In a thin-walled sample, at a distance of 3 mm from the substrate, the volume fraction of the Ti_2Ni phase was about 25%. As the height of samples increased, the volume fraction of the Ti_2Ni phase gradually decreased and was 5% at the top of the sample. The morphology of the Ti_2Ni phase was a cellular structure; the cell walls consisted of individual crystallites.

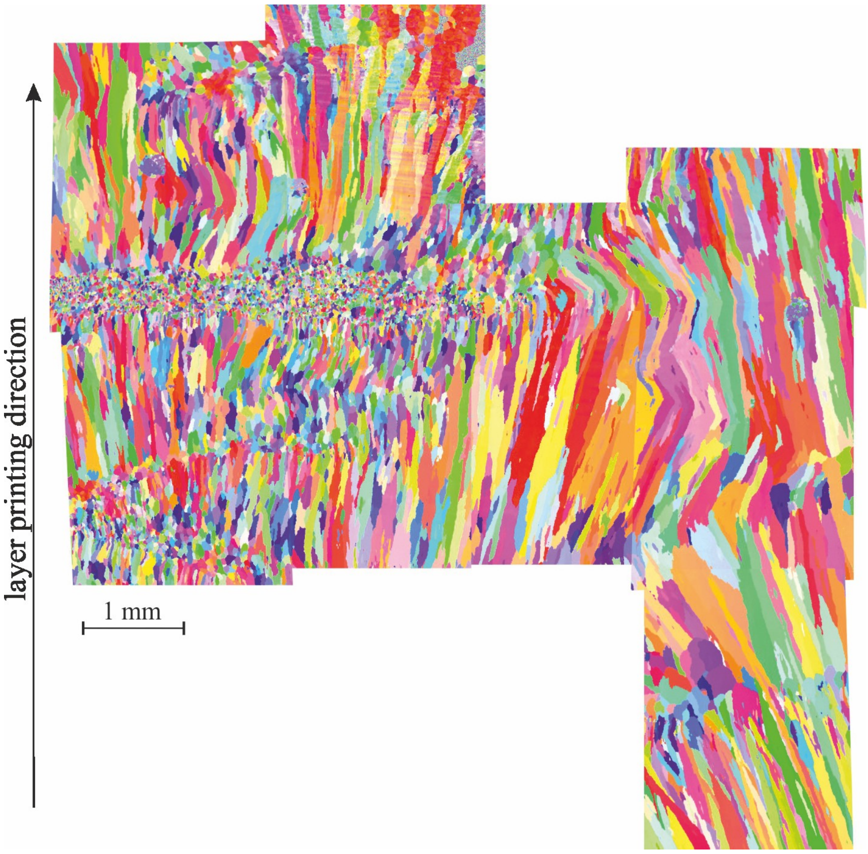

Fig. 1. The EBSD map of thin-walled samples obtained by the EBAM method.
The bottom boundary of the frame is located 1 mm from the substrate.

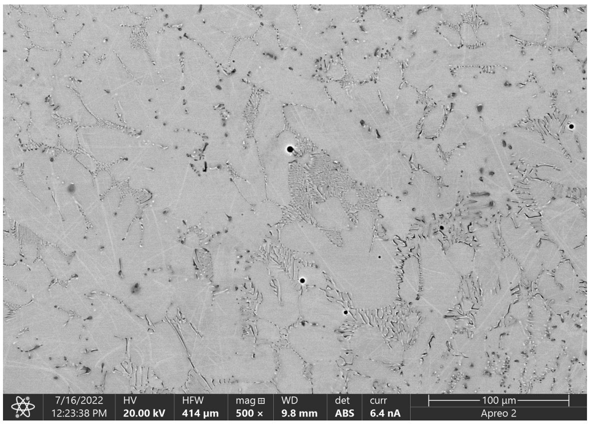

Fig. 2. Thin-walled sample. Image obtained by secondary electron method.

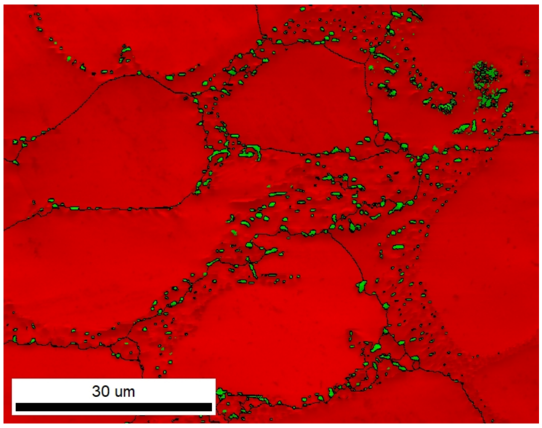

Fig. 3. Thin-walled sample. Phases map obtained by EBSD method.

The study of the bar-shaped samples showed that the microstructure remains qualitatively similar to the microstructure of thin-walled samples, Fig. 4 and 5. Inside the layers of the printed material, the samples have elongated grains, and at the boundaries of the layers there are quasi-equiaxed grains. In the bar-shaped sample, the volume fraction of the Ti_2Ni phase was larger and varied in height from 50% at a distance of 3 mm from the substrate to 15% at the top of the sample. In the bar-shaped sample, the grains of the Ti_2Ni phase had an equiaxial shape. Based on the obtained results, it can be assumed that printing samples using a strategy that involves contact with a larger area of the substrate leads to increased diffusion of substrate atoms into the sample compared to thin-walled samples.

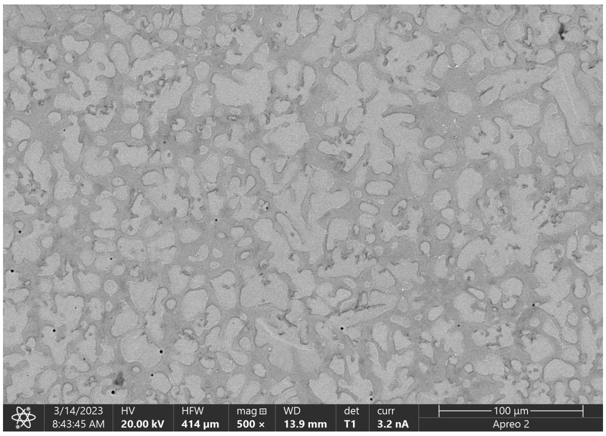

Fig. 4. Bar-shaped sample. Image obtained by secondary electron method.

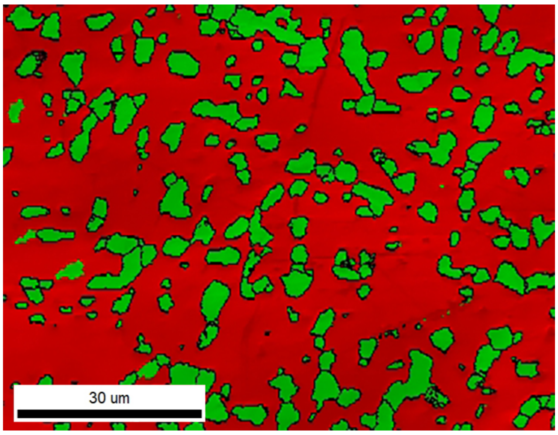

Fig. 5. Bar-shaped sample. Phases map obtained by EBSD method.

3.2. Mechanical properties

To evaluate the mechanical properties of TiNi-based alloy samples printed by the EBAM method on a titanium substrate, Vickers microhardness studies were carried out (indenter load was 490 N). In the initial coarse-grained homogeneous samples of the $Ti_{49.3}Ni_{50.7}$ (at.%) alloy, the microhardness is (2.25±0.10) GPa [3]. The formation of the Ti_2Ni phase particles leads to strengthening and embrittlement of the studied samples material, Table 1. It can be seen that the material of the samples near the substrate has a higher hardness. As the distance from the substrate increases and consequently the fraction of the Ti_2Ni phase decreases, the microhardness value decreases and approaches the characteristics of the initial coarse-grained homogeneous samples. It should be noted that the bar-shaped sample material exhibits higher hardness than the material of thin-walled samples. This correlates with the studies of the structural-phase state, indicating a higher substrate atoms diffusion into the “body” of the samples with increasing contact area with the substrate.

Table 1. The values of microhardness of samples depending on the printing strategy.

	Bottom (near substate)	Central region	Top
Thin-walled	3.58±0.41	2.93±0.37	2.56±0.35
Bar-shaped	5.21±0.47	3.16±0.40	2.63±0.35

3.3. Discussion

Thus, it is shown that the studied samples, regardless of the strategy used, have a heterogeneous coarse-grained microstructure. At room temperature, all studied samples consist of the B2 phase of the TiNi and the Ti_2Ni phase. In the thin-walled sample, the volume fraction of the Ti_2Ni phase is ~ 2 times lower than in the bar-shaped sample. As the height of the samples increased, the volume fraction of the Ti_2Ni phase gradually decreased and at the top of the sample it was 5% and 15% for thin-walled and bar-shaped samples, respectively. It was established that in the case of a thin-walled sample, the morphology of the Ti_2Ni phase was a cellular structure (the cell walls consisted of individual crystallites). In the bar-shaped sample, the grains of the Ti_2Ni phase had an equiaxial shape.

It should be noted that according to [8, 10], at room temperature, samples printed on a titanium substrate are predominantly in the state of the B19' martensitic phase. The main difference between the results of this work is that, regardless of the strategy used, the printed samples at room temperature have a B2 phase structure. We assume that this structural-phase state is a consequence of the gradual cooling of the studied samples in a vacuum chamber. According to the thermal imager data, at the end of printing, the sample had a temperature of at least 800°C. Probably, this led to the gradual precipitation of the Ti_2Ni phase throughout the entire volume of the material, as a result of which the composition of the matrix began to approach the composition of the wire.

Based on the obtained results, it can be assumed that printing samples using a strategy that involves contact with a larger area of the substrate leads to increased diffusion of substrate atoms into the sample compared to thin-walled samples.

4. Conclusion

It is shown that the most optimal approach for TiNi printing via the EBAM method on a titanium substrate is to print the alloy in the form of thin-walled samples. TiNi printing according to the strategy, when contact with a larger substrate area is assumed, results in a disproportionately increased diffusion of substrate atoms into the sample, in comparison to thin-walled samples. This, in turn, leads to an increase in the volume fraction of the Ti_2Ni phase. It was found that, irrespective of the printing strategy employed, the volume fraction of the Ti_2Ni phase decreases with increasing distance from the substrate, and the microhardness values of the samples, which are closest to those of the original wire, are observed in the upper part of the samples.

Acknowledgement

The work was supported by a grant of the Russian Science Foundation Project No. 24-29-00598.

5. References

[1] J.M. Jani, M. Leary, A. Subic, and M.A. Gibson, A review of shape memory alloy research, applications and opportunities, *Materials & Design*, vol. **56**, 1078, 2014; doi: 10.1016/j.matdes.2013.11.084

[2] Q. Chen and G.A. Thouas, Metallic implant biomaterials, *Materials Science and Engineering R*, vol. **87**, 1, 2015; doi: 10.1016/j.mser.2014.10.001

[3] K. Otsuka and X. Ren, Physical metallurgy of Ti-Ni-based shape memory alloys, *Progress in Materials Science*, vol. **50**, 511, 2005; doi: 10.1016/j.pmatsci.2004.10.001

[4] E. Kaya and I. Kaya, A review on machining of NiTi shape memory alloys: the process and post process perspective, *The International Journal of Advanced Manufacturing Technology*, vol. **100**, 2045, 2019; doi: 10.1007/s00170-018-2818-8

[5] H. Meier, C. Haberland, and J. Frenzel, Structural and Functional Properties of NiTi Shape Memory Alloys Produced by Selective Laser Melting, *Innovative Developments in Design and Manufacturing: Advanced Research in Virtual and Rapid Prototyping*, 291, 2011; doi: 10.1201/b11341-47

[6] C. Haberland, M. Elahinia, J.M. Walker, H. Meier and J. Frenzel, On the development of high quality NiTi shape memory and pseudoelastic parts by additive manufacturing, *Smart Materials and Structures*, vol. **23**, 104002, 2014; doi: 10.1088/0964-1726/23/10/104002

[7] P.R. Halani, I. Kaya, Y.C. Shin, and H.E. Karaca, Phase transformation characteristics and mechanical characterization of nitinol synthesized by laser direct deposition, *Materials Science and Engineering A*, vol. **559**, 836, 2013; doi: 10.1016/j.msea.2012.09.031.

[8] B. Li, L. Wang, B. Wang, D. Li, R. Cui, B. Su, L. Yao, L. Luo, R. Chen, Y. Su, J. Guo, and H. Fu, Solidification characterization and its correlation with the mechanical properties and functional response of NiTi shape memory alloy manufactured by electron beam freeform fabrication, *Additive Manufacturing*, vol. **48**, 102468, 2021; doi: 10.1016/j.addma.2021.102468

[9] B. Li, L. Wang, B. Wang, D. Li, J. P. Oliveira, R. Cui, J. Yu, L. Luo, R. Chen, Y. Su, J. Guo, and H. Fu, Tuning the microstructure, martensitic transformation and superelastic properties of EBF^3-fabricated NiTi shape memory alloy using interlayer remelting, *Materials & Design*, vol. **220**, 110886, 2022; doi: 10.1016/j.matdes.2022.110886
[10] G. Chen, Y. Ma, X. Teng, J. Liu, B. Zhang, and J. Cao, Microstructure evolution and shape memory function mechanism of NiTi alloy by electron beam 4D printing, *Applied Materials Today*, vol. **31**, 101749, 2023; doi: 10.1016/j. apmt.2023.101749
[11] N.N. Resnina, I.A. Palani, P.S. Liulchak, S.P. Belyaev, S.S. Mani Prabu, S. Jayachandran, and V.D. Kalganov, Structure of a 3D frame-bridge NiTi sample deposited on a low carbon steel substrate by wire arc additive manufacturing, *Letters on Materials*, vol. **10**, 496, 2020; doi: 10.22226/2410-3535-2020-4-496-500
[12] N. Resnina, I.A. Palani, S. Belyaev, S. Singh, P. Liulchak, U. Karaseva, S.S. Mani Prabu, S. Jayachandran, V. Kalganov, E. Iaparova, and E. Demidova, Influence of heat treatment on the structure and martensitic transformation on NiTi alloy produced by wire arc additive manufacturing, *Materialia*, vol. **20**, 101238, 2021; doi: 10.1016/j.mtla.2021.101238